Electron Transfer Reaction from Triplet 1,4-Dimethoxybenzene to Hydronium Ion in Aqueous Solution

So Tajima, Seiji Tobita,* and Haruo Shizuka*

Department of Chemistry, Gunma University, Kiryu, Gunma 376-8515, Japan

Received: March 3, 1999; In Final Form: May 24, 1999

The electron transfer (ET) reaction from the triplet state of 1,4-dimethoxybenzene (^{3}DMB*) to the hydronium ion (H_{aq}^+) in aqueous solution at 295 K was studied by means of the laser photolysis method. ^{3}DMB* was quenched by H_{aq}^+ and D_{aq}^+ with the quenching rate constants of 7.7 ($\pm$0.4) $\times$ 10^6 and 2.6 ($\pm$0.4) $\times$ 10^6 M^{-1} s^{-1}, respectively. The occurrence of the ET reaction was substantiated by formation of a DMB cation radical ($DMB^{+\bullet}$) coinciding with disappearance of ^{3}DMB*. From kinetic analyses, the rate constant (k_{et}^H) for the ET reaction from ^{3}DMB* to H_{aq}^+ was determined to be 7.5 ($\pm$0.4) $\times$ 10^6 M^{-1} s^{-1}. The observed ET rate exhibited a significantly smaller value compared to the diffusion-controlled rate in aqueous solution. The free energy changes for the ET reaction were estimated to be +28 and −175 kJ mol^{-1} for the reactions ^{3}DMB* + H_{aq}^+ → $DMB^{+\bullet}$ + H and ^{3}DMB* + H_{aq}^+ → $DMB^{+\bullet}$ + 1/2H_2, respectively. The observed small ET rate constant (7.5 ($\pm$0.4) $\times$ 10^6 M^{-1} s^{-1}) revealed that the ET corresponds to the former reaction. The large isotope effect (k_{et}^H/k_{et}^D = 3.0) was observed for the ET reaction between ^{3}DMB* and H_{aq}^+ (or D_{aq}^+). The fluorescence of DMB was also quenched by H_{aq}^+ with a quenching rate constant of 6.2 ($\pm$0.4) $\times$ 10^7 M^{-1} s^{-1}. The singlet quenching was similarly ascribable to the ET reaction from ^{1}DMB* to the hydronium ion.

1. Introduction

The properties of the proton such as transport in liquid water and chemical reactivity are of essential importance for the understanding of chemical and biological phenomena in water.[1] One remarkable property of the proton lies in its anomalously large mobility in aqueous solution. Recently, a number of theoretical studies by using molecular dynamics (MD) calculations and also ab initio calculations have been carried out to clarify the mechanism of proton transport.[2−8] Reactivity of the proton is also an important subject not only from fundamental aspects in chemistry but also in elucidating the primary events occurring in radiolysis of cooling water of nuclear reactors.[9−12] In liquid water, the proton exists as a hydronium ion. Because of its large diffusion coefficient ($D(H_3O^+)$ = 9.0 $\times$ 10^{-9} m^2 s^{-1}),[9,12] the hydronium ion in water (H_{aq}^+) reacts very rapidly with primary products in radiolysis of water:[9−17]

$$H_{aq}^+ + OH^- \rightarrow H_2O \quad (1)$$

$$H_{aq}^+ + e_{aq}^- \rightarrow H_{aq} \quad (2)$$

Here, the reactions of H_{aq}^+ with OH^- and the hydrated electron (e_{aq}^-) can be regarded as the most fundamental proton- and electron-transfer reactions. The bimolecular reaction between H_{aq}^+ and OH^- is known to proceed with a diffusion-controlled rate (the rate constant is reported to be 1.12 $\times$ 10^{11} M^{-1} s^{-1}),[16] while the rate constant (k = 2.3 $\times$ 10^{10} M^{-1} s^{-1})[9,10,12] for the reaction between H_{aq}^+ and e_{aq}^- is reported to be much smaller than that of reaction 1, despite the similar diffusion coefficients of the hydrated electron ($D(e_{aq}^-)$ = 4.8 $\times$ 10^{-9} m^2 s^{-1})[12] and OH^- ($D(OH^-)$ = 5.0 $\times$ 10^{-9} m^2 s^{-1}).[9] Goulet and Jay-Gerin[10] have shown that the reaction probability per encounter, where one encounter consists of many collisions in the same cage of solvent molecules, is quite small for the reaction of e_{aq}^- with H_{aq}^+.

Reactivities of protons toward excited organic and inorganic molecules have also received much attention during past decades.[18−22] Acid−base equilibrium in the excited organic molecules such as aromatic amines, aromatic alcohols, and carboxylic acids has been an interesting subject because of dramatic changes of the acidity in the excited singlet state due to differences in electronic structures between ground and excited states.[18−21] For excited aromatic molecules with a significant intramolecular charge transfer character (e.g., 1-naphthol, 1-naphthylamine), not only proton association and dissociation on a substituent but also proton-induced fluorescence quenching processes are often observed.[20,21] This characteristic quenching mechanism due to the presence of protons has been revealed to occur as a result of electrophilic protonation to one of carbon atoms of the aromatic ring in the excited state.[20,21]

As mentioned above, the hydronium ion is known to act usually as a proton donor in chemical processes. In addition, it has been reported that photoinduced electron transfer from inorganic complexes to the hydronium ion to produce hydrogen molecule can be utilized for solar energy storage.[22] However, direct electron transfer reactions from excited organic molecules to the hydronium ion have not been reported under moderately acidic conditions.

The aim of the present study is to investigate the direct electron-transfer process from excited organic molecules to the hydronium ion with particular interest in the kinetics and thermochemistry. 1,4-Dimethoxybenzene (DMB) was chosen as a sample molecule, because it has a relatively large electron-donating ability and a relatively high solubility in water. The bimolecular rate constant was determined for the electron-transfer reaction from triplet DMB (^{3}DMB*) to the hydronium ion.

* Author to whom correspondence should be addressed. Telephone: 81-277-30-1210. Fax: 81-277-30-1213. E-mail: shizuka@chem.gunma-u.ac.jp.

10.1021/jp990743a CCC: $18.00
Published on Web 07/16/1999

2. Experimental Section

Materials. DMB (Wako), naphthalene (NP) (Wako), and benzophenone (BP) (Wako) were purified by vacuum sublimation. Aniline (AN) (Kanto) and 2,3-dimethyl-1,3-butadiene (Aldrich) were purified by vacuum distillation. Potassium hexacyanoferrate(II), 3-hydrate (KISHIDA, 99.5%) was used without further purification. Deionized water was purified by using a Millipore MILLI-Q-Labo. Cyclohexane (CH) (Aldrich, spectrophotometric grade) was treated on an alumina column prior to use. 3-Methylpentane (3MP) (Wako, GR grade) was dried with $CaCl_2$, refluxed over $LiAlH_4$, and then distilled. Acetonitrile (ACN) (Kanto) was purified by distillation. H_2SO_4 (Wako, 97%, S. S. Grade) and Cs_2SO_4 (Fluka, 99.9%) were used as received. D_2O (MERCK, 99.8%) and D_2SO_4 (Aldrich, 98% solution in D_2O, 99.5 atom % D) were used without further purification. The concentration of H_3O^+ or D_3O^+ of each aqueous solution was determined by a pH meter (Horiba F-8) calibrated at pH 4.00 (phthalate pH standard solution (Wako)) and pH 6.88 (phosphate pH standard equimolal solution (Wako)) at 293 K. H_2SO_4 was used to adjust the H_3O^+ concentration ($[H_3O^+]$) of sample solutions.

The concentration of DMB in each solution was maintained at $\sim 5 \times 10^{-4}$ and $\sim 1 \times 10^{-4}$ M for laser photolysis and fluorescence experiments, respectively. All sample solutions in a quartz cell with a 10 mm path length were thoroughly degassed by freeze−pump−thaw cycles on a high-vacuum line.

Methods. The absorption and fluorescence spectra were measured with a UV/vis spectrophotometer (JASCO, Ubest-50) and a spectrofluorometer (Hitachi, F-4010), respectively. The fluorescence lifetime (τ_f) was obtained with a time-correlated single-photon-counting fluorometer (Edinburgh Analytical Instruments, FL900CDT). This apparatus enabled us to measure both excitation and emission response functions, and to compute decay parameters by the deconvolution method using a nonlinear least-squares fitting. A nanosecond pulsed discharge lamp (pulse width 5 ns, repetition rate 40 kHz) filled with hydrogen gas was used as the excitation light source. Emission of samples was detected by a photomultiplier (Hamamatsu, R955) using the photon counting method.

The nanosecond laser flash photolysis experiments were carried out by using the third or fourth harmonics (355 or 266 nm) of a Nd^{3+}:YAG laser (Spectra-Physics GCR-130, pulse width 6 ns) as the excitation source. The monitoring system of transient species consisted of a pulsed xenon lamp (Ushio, UXL-151D), a monochromator (Ritsu, MC-20N), and a photomultiplier (Hamamatsu, R928). The timing sequence between the laser pulse and the xenon flash lamp was controlled by a digital delay pulse generator (Stanford Research Systems, Model DG-535). The transient signals were recorded on a digitizing oscilloscope (Tektronix, TDS-744; 500 MHz, 2×10^9 samples s^{-1}) and transferred to a personal computer (NEC, PC-9821Ap) to analyze the data. The signals were averaged over 5−10 laser shots to improve the signal-to-noise ratio. The laser power for each shot was monitored by a pyroelectric detector (Scientech, P25/S200). All sample solutions were exposed to less than 20 laser shots to avoid depletion of the starting materials and accumulation of possible photoproducts.

The quantum yield of intersystem crossing (Φ_{isc}) of DMB was obtained by means of the time-resolved thermal lensing (TRTL) method. The detection system of the TRTL signals has been reported elsewhere.[23] Briefly, the fourth harmonics (266 nm) of a Nd^{3+}:YAG laser (Spectra-physics GCR-130, pulse width 6 ns) was used as the excitation source. A cw He−Ne laser beam (NEC, GLG2026, 633 nm) was used as monitoring light. The probe beam was introduced into a monochromator (Jobin-Yvon, HR-10) after passing it through an optical filter and a small pinhole (Corion, 2401; 300 μm diameter). The intensity change of the probe light was detected by a photomultiplier (Hamamatsu, R928). The TRTL signals were recorded on a digitizing oscilloscope (Tektronix, TDS-744) and averaged over five hundred laser shots to improve the signal-to-noise ratio. The data were analyzed by a personal computer (NEC, PC-9821Ap).

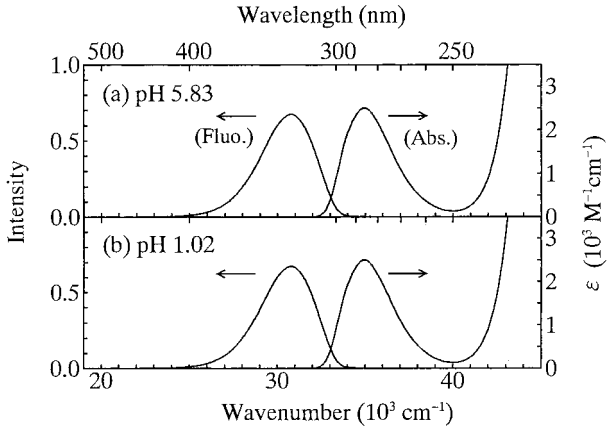

Figure 1. Absorption (Abs.) and fluorescence (Fluo.) spectra of DMB in aqueous solutions (a) pH 5.83 and (b) pH 1.02 at 295 K.

The fluorescence quantum yield was determined by using AN in CH ($\Phi_f = 0.17$ at 293 K) as an actinometer.[24] The quantum yield of transient species was determined by using NP in CH ($\Phi_{isc} = 0.75$[25] and $\epsilon = 24\,500$ M^{-1} cm^{-1} at 415 nm[26]) as an actinometer.

3. Results and Discussion

3.1. Absorption and Emission Spectra. Figure 1 shows the absorption and emission spectra of DMB in degassed H_2O solution at 295 K. The spectral shape and position under the acidic condition (pH 1.02) agree fairly well with those taken at pH 5.83. The absorption spectra showed no spectral change even under a high hydronium ion concentration (4.0 M), indicating that the ground-state protonation to DMB is negligible at $[H_3O^+] < 4.0$ M.

On the other hand, the fluorescence quantum yield (Φ_f) and fluorescence lifetime (τ_f) decreased moderately with increasing $[H_3O^+]$ and the fluorescence quenching rate constant (k_q) was obtained to be 6.2×10^7 M^{-1} s^{-1} from the Stern−Volmer plots:

$$\frac{\Phi_f^0}{\Phi_f} = \frac{\tau_f^0}{\tau_f} = 1 + k_q \tau_f^0 [H_3O^+] \qquad (3)$$

where Φ_f and Φ_f^0 denote the fluorescence quantum yields of DMB in aqueous solution with and without $[H_3O^+]$ and τ_f and τ_f^0 are the fluorescence lifetimes of DMB in aqueous solution with and without $[H_3O^+]$ at 295 K. τ_f^0 and Φ_f^0 are determined to be 1.71 (±0.01) ns and 0.11 in aqueous solution as listed in Table 1.

The k_q value obtained is much smaller than the diffusion-controlled rate constant ($k_d = 5.1 \times 10^{10}$ M^{-1} s^{-1}) estimated from the Smoluchowski equation:

$$k_d = 10^3 \times 4\pi r_{AB}\{D(H_3O^+) + D(\mathrm{DMB})\}N_A \qquad (4)$$

where $D(H_3O^+)$ and D(DMB) are the diffusion coefficients of the proton and DMB in aqueous solution, and N_A is the Avogadro constant. The effective collision radius (r_{AB}) is

TABLE 1: Fluorescence Quantum Yields (Φ_f^0) and Lifetimes (τ_f^0) of DMB in H_2O and D_2O, and the Fluorescence Quenching Rate Constant (k_q) Induced by H_{aq}^+ at 295 K

quencher	solvent	Φ_f^{0a}	τ_f^0(ns)	k_q (10^7 M^{-1} s^{-1})
H_{aq}^+	H_2O	0.11	1.71	6.2
D_{aq}^+	D_2O	0.11	1.72	

[a] Determined by using aniline in CH ($\Phi_f = 0.17$)[24] as an actinometer.

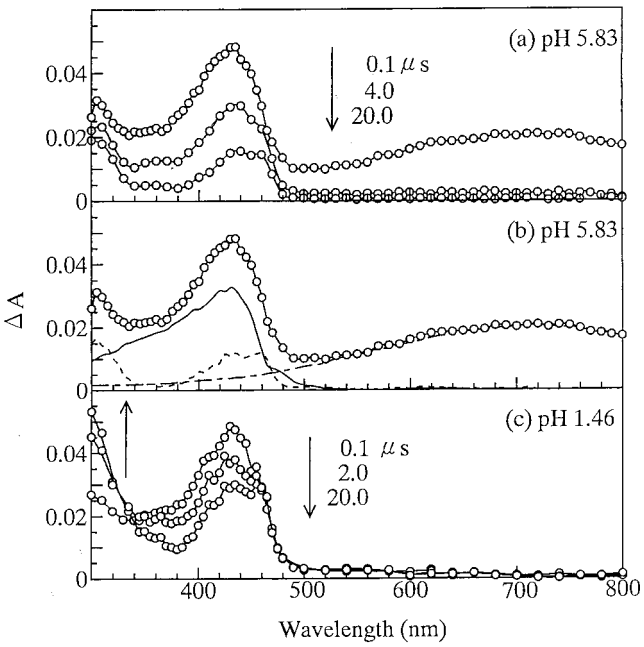

Figure 2. Transient absorption spectra obtained by 266 nm laser photolysis of DMB in aqueous solution at 295 K. (a) Time-resolved spectra at pH 5.83; (b) transient absorption spectra of DMB at the delay time of 0.1 μs, and absorption spectra of ^{3}DMB* (—), hydrated electron (—•—) and $DMB^{+\bullet}$ (---); (c) time-resolved absorption spectra at pH 1.46.

assumed to be 0.70 nm. The $D(H_3O^+)$ value is known to be 9.0×10^{-9} m^2 s^{-1}.[9,12] The value of D(DMB) is estimated by the following Stokes−Einstein equation

$$D = \frac{k_B T}{6\pi\eta r_s}$$

where k_B is the Boltzmann constant, T represents absolute temperature, η is the viscosity of solvent, and r_s is the radius of solute molecule. The r_s value of DMB is estimated to be 0.37 nm from the reported density for DMB (1.053×10^3 kg m^{-3}).[27] In the case of H_2O, the η value is 0.9579×10^{-2} N m^{-2} s at 295 K.[27] Therefore, the D(DMB) value is obtained to be 6.1×10^{-10} m^2 s^{-1} at 295 K. Thus the diffusion-controlled rate constant of the reaction between ^{1}DMB* and H_{aq}^+ can be calculated to be 5.1×10^{10} M^{-1} s^{-1}.

3.2. Triplet Formation. Figure 2a shows the transient absorption spectra obtained by 266 nm laser flash photolysis of DMB in degassed aqueous solution (pH 5.83) at 295 K.

The transient absorption spectrum of 0.1 μs after laser pulsing gives the main absorption bands at around 430 and 720 nm. Both bands were quenched appreciably by dissolved oxygen. The spectral feature of the band at 430 nm is similar to the $T_n \leftarrow T_1$ absorption spectrum of DMB in aqueous solution.[28] Laser photolysis of DMB in CH produced a similar band which was quenched by addition of a typical triplet quencher (2,3-dimethyl-1,3-butadiene) with a rate constant of 7.1×10^9 M^{-1} s^{-1} at 295 K. Hence, the absorption band at 430 nm in Figure 2a can

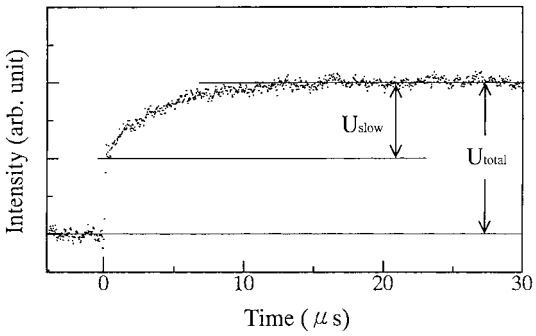

Figure 3. Time evolution of the TRTL signal of DMB in CH at 295 K.

be ascribed to the $T_n \leftarrow T_1$ absorption of DMB. The lifetime of the triplet DMB (^{3}DMB*) in aqueous solution was determined to be 5.5 μs at pH 5.83. The actual $T_n \leftarrow T_1$ absorption spectrum of DMB in aqueous solution was obtained by subtracting the absorption spectra of the hydrated electron and $DMB^{+\bullet}$ (discussed below) from that of DMB (pH 5.83) at delay time of 0.1 μs (Figure 2b).

The quantum yield of intersystem crossing (Φ_{isc}) of DMB in CH was determined by the TRTL method. The TRTL signal of DMB in CH is shown in Figure 3.

Since in CH *p*-methoxyphenoxy radical formation due to $O-CH_3$ bond fission in the S_1 state of DMB is involved, the intensity ratio (U_{slow}/U_{total}) between the slow rise component (U_{slow}) and the total TRTL signal (U_{total}) is given by[29−31]

$$\frac{U_{slow}}{U_{total}} = \frac{\Phi_{isc} E_T}{E_{ex} - \Phi_f \langle E_S \rangle - \Phi_R \Delta H} \qquad (6)$$

where E_{ex} and E_T are the excitation photon energy (450 kJ mol^{-1}) and the 0−0 transition energy of the lowest triplet state (T_1), respectively, and $\langle E_S \rangle$ is the average energy dissipated by fluorescence from the S_1 state. The U_{slow}/U_{total} value was estimated to be 0.50 (±0.02). The Φ_f value for DMB in CH at 295 K was determined as 0.13 (±0.01). The E_T value of DMB was determined as 325 kJ mol^{-1} from the 0−0 band of phosphorescence spectra of DMB in 3MP at 77 K. The quantum yield of the *p*-methoxyphenoxy radical formation (Φ_R) was determined as 0.11 in CH by using the ϵ value (5550 M^{-1} cm^{-1} at 403 nm).[32] The enthalpy change (ΔH) for the *p*-methoxyphenoxy radical formation was estimated from the $O-CH_3$ bond energy of anisole as 238 kJ mol^{-1}.[33] From these photophysical values, Φ_{isc} of DMB in CH was determined to be 0.58 ± 0.02.

The triplet−triplet absorption coefficient (ϵ_T) of ^{3}DMB* in CH solution was determined to be 3700 M^{-1} cm^{-1} at 430 nm by use of the $T_n \leftarrow T_1$ absorption of NP in CH as an external actinometer ($\Phi_{isc} = 0.75$[25] and $\epsilon_T = 24\,500$ M^{-1} cm^{-1} at 415 nm[26]). This ϵ_T value is close to the reported value in ethanol (3300 M^{-1} cm^{-1} at 420 nm).[28] Since the spectral shape of the $T_n \leftarrow T_1$ spectrum of DMB in aqueous solution was similar to that in CH, the ϵ_T value in aqueous solution was assumed to be the same as that in CH in the following analyses.

3.3. Direct Photoionization of DMB in Aqueous Solution. The broad absorption band at around 720 nm in Figure 2a can be assigned to the hydrated electron (e_{aq}^-) from the characteristic spectral shape.[34] After disappearance of the $T_n \leftarrow T_1$ and e_{aq}^- absorption bands, a longer-lived component with band maxima at 435 and 460 nm can be seen in Figure 2a. The spectral feature of this band is in agreement with that of the DMB cation radical ($DMB^{+\bullet}$).[28,35] The absorbance decreased according to the first-order kinetics, with a lifetime of 160 μs under the present

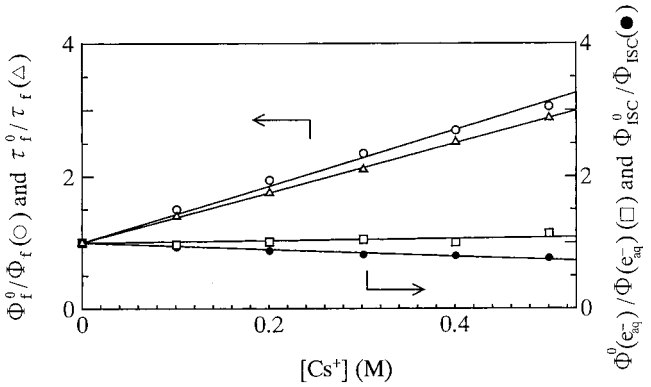

Figure 4. Plots of Φ_f^0/Φ_f (circles) and τ_f^0/τ_f (triangles), $\Phi^0(e_{aq}^-)/\Phi(e_{aq}^-)$ (squares), and Φ_{isc}^0/Φ_{isc} (solid circles) of DMB as a function of $[H_3O^+]$ in aqueous solution at 295 K.

experimental condition. Figure 2b shows the absorption spectra of e_{aq}^-, $DMB^{+\bullet}$, and $^3DMB^*$.

The results of laser flash photolysis of DMB in aqueous solution clearly show the occurrence of photoelectron ejection from excited DMB to water, resulting in the formation of $DMB^{+\bullet}$ and e_{aq}^-:

$$DMB + h\nu\ (266\ nm) \rightarrow DMB^{+\bullet} + e_{aq}^- \qquad (7)$$

The observed e_{aq}^- concentration showed quadratic laser power dependences under the laser pulse energies of 1−15 mJ pulse^{-1} cm^{-2}, indicating that the photoionization of DMB in aqueous solution takes place via two-photon absorption processes. It is noteworthy here that aniline and its derivatives can be ionized by one photon absorption under almost the same experimental condition.[36,37]

The Cs^+ ion is known as an effective singlet quencher in aqueous solution.[38] The quenching in the excited singlet state of aromatic compounds by Cs^+ is usually caused by the external heavy atom effect, resulting in the enhancement of intersystem crossing. If the absorption of the second photon occurs through relaxed S_1 states of DMB, then the e_{aq}^- yield should decrease with increasing Cs^+ concentration ($[Cs^+]$). While, if the second absorption occurs from the T_1 state, then the e_{aq}^- yield should increase with increasing $[Cs^+]$. Figure 4 shows the plots of Φ_f^0/Φ_f, τ_f^0/τ_f, Φ_{isc}^0/Φ_{isc}, and $\Phi^0(e_{aq}^-)/\Phi(e_{aq}^-)$ as a function of $[Cs^+]$ for DMB in aqueous solution.

Here Φ_{isc} and Φ_{isc}^0 are the quantum yields of intersystem crossing with and without Cs^+, respectively. The Φ_f and τ_f values are reduced by addition of Cs^+, while the Φ_{isc} value shows an increase upon addition of Cs^+. The fluorescence quenching rate constants (k_q) are obtained to be 2.6×10^9 and 2.2×10^9 M^{-1} s^{-1} for the (Φ_f^0/Φ_f) and (τ_f^0/τ_f) plots, respectively. However, the $\Phi(e_{aq}^-)$ value is not affected by Cs^+, suggesting that the second absorption process occurs through the nonrelaxed S_1 state ($S_1^\dagger$) of DMB.

The ionization potential (IP_{liq}) of a solute molecule in solution is usually expressed as[39,40]

$$IP_{liq} = IP_{gas} + P_+ + V_0 \qquad (8)$$

where IP_{gas} is the ionization potential of a solute molecule in the gas phase, P_+ is the adiabatic electronic polarization energy of the medium by the positive ion, and V_0 is the minimum energy of a quasi-free electron in the liquid relative to an electron in the gas phase. The IP_{gas} of DMB is reported to be 7.535 and 7.508 eV for the cis and trans isomers, respectively,[41] which are significantly smaller than that (9.24 eV) of benzene[42] owing to the presence of electron-donating methoxy groups. Recently, we have reported that aqueous aniline (IP_{gas} = 7.72 eV) and its para-substituted derivatives undergo one-photon ionization from the nonrelaxed S_1 state upon 266 nm excitation.[36,37] The photoionization yields showed a good correlation with an extent of charge localization in the cation state rather than the magnitude of IP_{gas}, indicating that polarization stabilization of the cation is an important factor to determine the photoionization yield. Despite its low IP_{gas} value, DMB showed predominantly a two-photon ionization mechanism. This would be due, at least in part, to delocalization of positive charge in the DMB cation, which results in a decrease of the polarization stabilization of the cation.

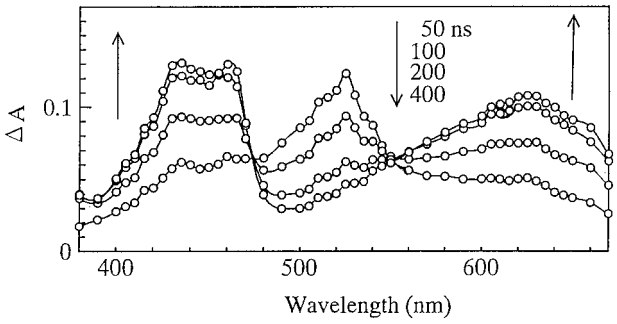

Figure 5. Transient absorption spectra obtained by 355 nm laser photolysis of the BP-DMB system in ACN−H_2O (4:1 v/v).

The molar absorption coefficient (ϵ_{rad}) of $DMB^{+\bullet}$ was determined by utilizing an electron-transfer reaction from DMB to triplet benzophenone ($^3BP^*$).[43] Figure 5 shows the time-resolved transient absorption spectra obtained by 355 nm laser photolysis of BP (5.7×10^{-3} M) and DMB (2.6×10^{-3} M) in ACN−H_2O (4:1 v/v).

The transient absorption spectrum at 520 nm observed at delay time of 50 ns is ascribable to the $T_n \leftarrow T_1$ absorption of BP in polar solvent.[43] With the lapse of time, the $T_n \leftarrow T_1$ absorption of BP decreases in intensity according to the first-order kinetics to give the residual absorption bands with the peaks at around 450 and 630 nm with isosbestic points at 475 and 550 nm. The residual absorption spectrum was reproduced by superposing those of the benzophenone anion radical[43] and $DMB^{+\bullet}$ in a 1:1 concentration ratio. The spectral changes in Figure 5 demonstrate that electron transfer occurs from DMB to $^3BP^*$ to produce $DMB^{+\bullet}$ and $BP^{-\bullet}$. Hence, the ϵ_{rad} for $DMB^{+\bullet}$ can be determined to be 6400 M^{-1} cm^{-1} at 435 nm by using the ϵ value (5700 M^{-1} cm^{-1} at 630 nm)[43] of benzophenone anion radical as reference. Our ϵ_{rad} value for $DMB^{+\bullet}$ is found to be significantly smaller than that (9040 M^{-1} cm^{-1} at 430 nm)[44] determined by the pulse radiolysis method.

3.4. Electron-Transfer Reaction from ^{3}DMB* to the Hydronium Ion. The transient absorption spectra taken by 266 nm laser flash photolysis of DMB in acidic aqueous solution (pH 1.46) at 295 K are shown in Figure 2c. The absorption spectrum at 0.1 μs after laser pulsing gives a main absorption band at 430 nm. The spectral shape and intensity are similar to that of $^3DMB^*$ obtained at pH 5.83 (Figure 2a). The broad absorption band due to e_{aq}^- is not seen because of rapid bimolecular reaction of e_{aq}^- with H_{aq}^+.[9,10,12] The transient absorption band remaining after disappearance of $^3DMB^*$ is in agreement with that of $DMB^{+\bullet}$. It is noteworthy here that the decay rate of $^3DMB^*$ increases with an increase of H_3O^+ concentration and that the absorbance (ΔA) of $DMB^{+\bullet}$ at the delay time of 20 μs becomes almost twice as large as that obtained at pH 5.83 under the same laser intensity. This shows that the total cation radical yield is enhanced by addition of

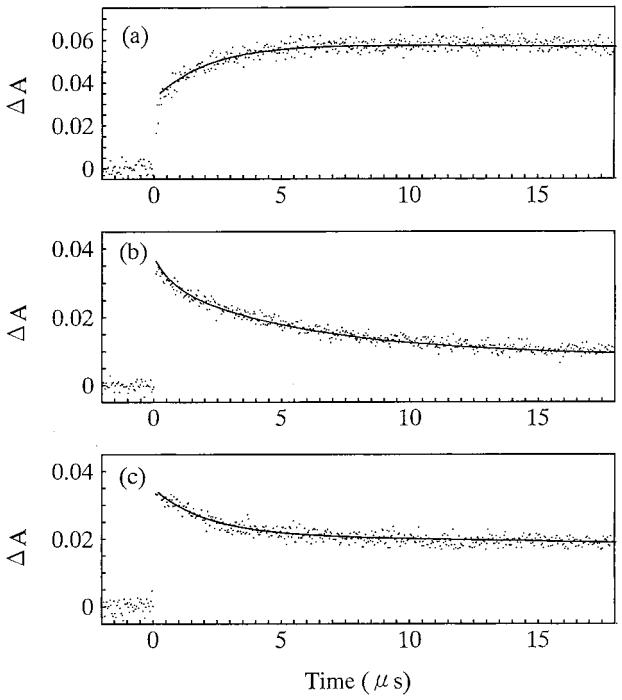

Figure 6. Time traces of the transient absorption spectra obtained by 266 nm laser photolysis of DMB in aqueous solution (a) pH 1.46 at 300 nm, (b) pH 5.83 at 400 nm, and (c) pH 1.46 at 400 nm.

acids, and suggests that electron transfer (ET) reaction from ^{3}DMB* to H_{aq}^+ occurs under acidic conditions.

One possible explanation of the enhancement of $DMB^{+\bullet}$ yield in the presence of acids might lie in reduction of recombination yield between $DMB^{+\bullet}$ and e_{aq}^- under high hydronium ion concentrations, because the hydronium ion reacts very rapidly with e_{aq}^- ($k = 2.3 \times 10^{10}$ M^{-1} s^{-1}).[9,10,12] However, judging from the low initial concentration of $DMB^{+\bullet}$ ($\sim 3 \times 10^{-6}$ M) and the short lifetime (1.3 μs) of e_{aq}^-, the recombination yield can be assumed to be negligible under the present experimental conditions. Therefore, it seems reasonable to assume that the ET reaction from ^{3}DMB* to H_{aq}^+ occurs under highly acidic conditions. In Figure 2c, one can see a rise component at around 300 nm due to slow formation of $DMB^{+\bullet}$, and the time profile at 300 nm is depicted in Figure 6a. The production of $DMB^{+\bullet}$ coinciding with the decay rate of ^{3}DMB* supports the involvement of the ET reaction from ^{3}DMB* to H_{aq}^+.

Figure 6, parts b and c, shows the time traces at 400 nm of the transient absorption spectra of DMB in aqueous solution taken at pH 5.83 ($[H_3O^+] = 1.48 \times 10^{-6}$ M) and pH 1.46 ($[H_3O^+] = 3.5 \times 10^{-2}$ M). The time profile consists of three decay components, ^{3}DMB*, $DMB^{+\bullet}$, and e_{aq}^-. Therefore, the time-dependent absorbance change ($\Delta A(t)$) monitored at 400 nm can be represented by the following equation:

$$\Delta A(t) = [^3\mathrm{DMB}^*]_0\, \epsilon_T^{400} \exp(-k_T^0 t) + [\mathrm{DMB}^{+\bullet}]_0\, \epsilon_{rad}^{400} \exp(-k_R^0 t) + [e_{aq}^-]_0\, \epsilon_{HE}^{400} \exp(-k_{HE}^0 t) \quad (9)$$

Here, the initial concentration of e_{aq}^- ($[e_{aq}^-]_0$), which can be assumed to be equal to $[DMB^{+\bullet}]_0$, is determined to be 3.5 ($\pm$0.2) $\times 10^{-6}$ M from the initial absorbance and the molar absorption coefficient of e_{aq}^- ($\epsilon_{HE} = 18\,500$ M^{-1} cm^{-1} at 720 nm).[45] The ϵ_T and ϵ_{rad} at 400 nm were estimated as 3100 and 2700 M^{-1} cm^{-1}, respectively, by using $\epsilon_T = 3700$ M^{-1} cm^{-1} at 430 nm and $\epsilon_{rad} = 6400$ M^{-1} cm^{-1} at 435 nm. To determine the ϵ_{HE} value at 400 nm, the transient absorption spectra of e_{aq}^- was taken by 266 nm photoionization of $Fe(CN)_6^{4-}$ in aqueous solution, and the ϵ_{HE} value at 400 nm was determined to be 2140 M^{-1} cm^{-1}. $[^3DMB^*]_0$ and $[DMB^{+\bullet}]_0$ in eq 9 represent the initial concentrations of ^{3}DMB* and $DMB^{+\bullet}$. $[^3DMB^*]_0$ was obtained as 7.5 ($\pm$0.5) $\times 10^{-6}$ M from the time profile in Figure 6b. In eq 9, k_T^0, k_R^0, and k_{HE}^0 are the decay rate constants of ^{3}DMB*, $DMB^{+\bullet}$, and e_{aq}^-, respectively. The value of k_{HE}^0 was determined from the single-exponential decay at 720 nm as 7.7 ($\pm$0.2) $\times 10^5$ s^{-1}. Since the cation radical ($DMB^{+\bullet}$) has a much longer lifetime compared to those of ^{3}DMB* and e_{aq}^-, the k_R^0 value was obtained to be 6.0 ($\pm$1.5) $\times 10^3$ s^{-1}. Hence, analyses of the time profile in Figure 6b enabled us to determine the k_T^0 value to be 1.8 ($\pm$0.2) $\times 10^5$ s^{-1}. The calculated decay curve (solid line in Figure 6b) by substituting the above photophysical parameters into eq 9 reproduces satisfactorily the experimental time profile.

SCHEME 1

$$^3\mathrm{DMB}^* + H_{aq}^+ \xrightarrow{k_{et}} \mathrm{DMB}^{+\bullet} + H_{aq} \quad (I)$$

$$^3\mathrm{DMB}^* + H_{aq}^+ \xrightarrow{k_q'} \mathrm{DMB} + H_{aq}^+ \quad (II)$$

Under acidic conditions, the $DMB^{+\bullet}$ yield and the decay rate of ^{3}DMB* increase with increasing H_3O^+ concentration. As a result, one can assume a reaction scheme for the triplet state as shown in Scheme 1, where k_{et} is the bimolecular rate constant for the ET reaction from ^{3}DMB* to H_{aq}^+, k_q' is the induced quenching rate constant of ^{3}DMB* by H_{aq}^+.

The sum of k_{et} and k_q' corresponds to the total quenching rate constant k_q^T. According to Scheme 1, the absorbance change monitored at 400 nm can be expressed by the following equation:

$$\Delta A(t) = [^3\mathrm{DMB}^*]_0 \epsilon_T^{400} \exp\{-(\tau_T)^{-1} t\} + [\mathrm{DMB}^{+\bullet}]_0 \epsilon_{rad}^{400} \exp(-k_R^0 t) + [^3\mathrm{DMB}^*]_0 \phi_{et} \epsilon_{rad}^{400} [\exp(-k_R^0 t) - \exp\{-(\tau_T)^{-1} t] \quad (10)$$

where ϕ_{et} ($= k_{et}[H_3O^+]/(k_T^0 + k_q^T[H_3O^+])$) stands for the efficiency of the ET reaction from ^{3}DMB* to H_{aq}^+ and τ_T ($= (k_T^0 + k_q^T [H_3O^+])^{-1}$) is the lifetime of ^{3}DMB* in the presence of H_{aq}^+. Here, the first term of the right-hand side in eq 10 shows the decay of ^{3}DMB*, the second term corresponds to the decay of $DMB^{+\bullet}$ produced by direct photoionization of DMB, and the third term represents the rise and decay of $DMB^{+\bullet}$ produced by the ET reaction. In eq 10, the decay term of e_{aq}^- is neglected, because the decay rate (8.1×10^8 s^{-1}) estimated from the bimolecular reaction rate (2.3×10^{10} M^{-1} s^{-1}) [9,10,12] between e_{aq}^- and H_{aq}^+ is much greater than that (4.6×10^5 s^{-1}) of ^{3}DMB* at $[H_3O^+] = 3.5 \times 10^{-2}$ M. The solid curves in Figure 6a,c were obtained by fitting eq 10 to the experimental values, where τ_T and ϕ_{et} were used as fitting parameters. The best-fitted values for τ_T and ϕ_{et} were 4.6 ($\pm$0.4) $\times 10^5$ s^{-1} and 0.50 ($\pm$0.05) at $[H_3O^+] = 3.5 \times 10^{-2}$ M.

To determine the ET rate constant between ^{3}DMB* and H_{aq}^+, the lifetime analyses of ^{3}DMB* as shown above were carried out under different H_3O^+ concentrations. Figure 7 shows the Stern−Volmer plots of τ_T^0/τ_T as a function of $[H_3O^+]$ for DMB in aqueous solution at 295 K, where τ_T and τ_T^0 are the lifetimes of ^{3}DMB* with and without H_{aq}^+.

From the slope of the straight line, the k_q^T value was determined to be 7.7 ($\pm$0.4) $\times 10^6$ M^{-1} s^{-1} for H_{aq}^+. Similar experiments were also carried out for the DMB/D_{aq}^+ system in

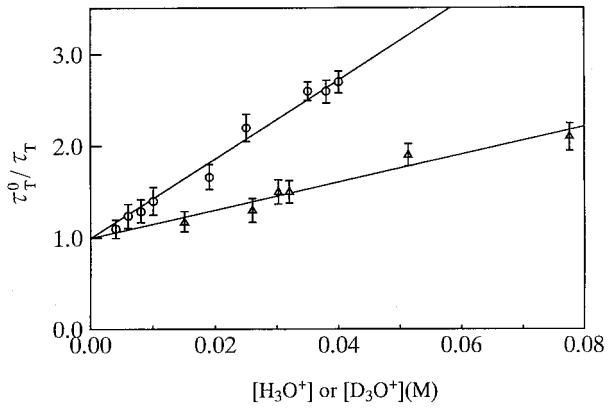

Figure 7. Plots of τ_T^0/τ_T of DMB as a function of $[H_3O^+]$ (circles) and $[D_3O^+]$ (triangles) in aqueous solution at 295 K.

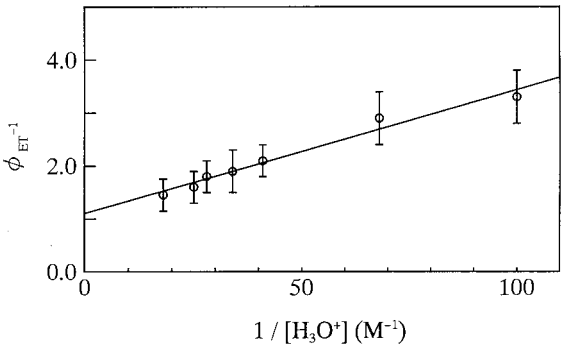

Figure 8. Plots of ϕ_{et}^{-1} as a function of $1/[H_3O^+]$ in aqueous solution at 295 K.

TABLE 2: Rate Constants for Triplet Quenching (k_q^T) and Electron Transfer (k_{et}) at 295 K

quencher	solvent	k_q^T (10^6 M^{-1} s^{-1})	k_{et} (10^6 M^{-1} s^{-1})	k_{et}/k_q^T
H_{aq}^+	H_2O	7.7	7.5	0.97
D_{aq}^+	D_2O	2.6	2.5[a]	0.97

[a] The value estimated by assuming $k_{et}/k_q^T = 0.97$.

D_2O, and the k_q^T value for D_{aq}^+ was obtained as 2.6 ($\pm$0.4) $\times$ 10^6 M^{-1} s^{-1} from the straight line in Figure 7.

The efficiency of the ET reaction (ϕ_{et}) is given by

$$\phi_{et} = \frac{[DMB^{+\bullet}]_{max}}{[^3DMB^*]_0} = \frac{k_{et}[H_3O^+]}{k_T^0 + k_q^T[H_3O^+]} \qquad (11)$$

where $[DMB^{+\bullet}]_{max}$ is the concentration of $DMB^{+\bullet}$ produced by the ET reaction from $^3DMB^*$ to H_{aq}^+, which is evaluated by subtracting $[DMB^{+\bullet}]$ produced by the direct photoionization from total $[DMB^{+\bullet}]$. Equation 11 can be rewritten as follows

$$\phi_{et}^{-1} = \frac{[^3DMB^*]_0}{[DMB^{+\bullet}]_{max}} = \frac{k_T^0}{k_{et}}\frac{1}{[H_3O^+]} + \frac{k_q^T}{k_{et}} \qquad (11')$$

Figure 8 shows plots of ϕ_{et}^{-1} against $1/[H_3O^+]$ for aqueous DMB at 295 K. From the slope of the straight line, the k_{et} value is determined to be 7.5 ($\pm$0.4) $\times$ 10^6 M^{-1} s^{-1} for H_{aq}^+.

The kinetic parameters obtained for the ET reaction from $^3DMB^*$ to H_{aq}^+ are summarized in Table 2. The proportion of k_{et} to k_q^T is obtained as 0.97 for H_{aq}^+, showing that the ET reaction from $^3DMB^*$ to the hydronium ion predominates in the triplet quenching of DMB by H_{aq}^+. If we assume the same k_{et}/k_q^T value for D_{aq}^+, k_{et} for D_{aq}^+ is estimated to be 2.5 $\times$ 10^6 M^{-1} s^{-1}, and the isotope effect (k_{et}^H/k_{et}^D) is obtained as 3.0.

3.5. Kinetics of the ET Reaction between ^{3}DMB* and H_{aq}^+. Transient absorption measurements of DMB in aqueous solution showed that the photoinduced ionization of DMB in acidic aqueous solution involves two different mechanisms: the photoelectron ejection to water by two-photon absorption (eq 7), and the ET reaction from excited $^3DMB^*$ to H_{aq}^+ (Scheme 1).

The elementary processes of the ET reaction can be divided into three steps:

$$^3DMB^* + H_{aq}^+ \underset{k_{-d}}{\overset{k_d}{\rightleftharpoons}} (^3DMB^*\cdots H_{aq}^+) \underset{k_{-e}}{\overset{k_e}{\rightleftharpoons}} (DMB^{+\bullet}\cdots H) \xrightarrow{k_{sep}} DMB^{+\bullet} + H_{aq} \qquad (12)$$

where k_d is the diffusion rate constant, k_{-d} is the dissociation rate constant, k_e and k_{-e} denote the rate constants for the forward and back electron transfers, respectively, and k_{sep} stands for the rate constant for separation of $(DMB^{+\bullet}\cdots H)$ to $DMB^{+\bullet}$ and H_{aq}. In the first step, $^3DMB^*$ and H_{aq}^+ diffuse together to form an outer-sphere encounter complex ($^3DMB^*\cdots H_{aq}^+$) with a rate constant of k_d which corresponds to the diffusion-controlled rate. In the second step, the encounter complex undergoes reorganization toward the transition state in which ET takes place to form a successor complex ($DMB^{+\bullet}\cdots H$). Finally, the successor complex dissociates to form the products.

By applying the steady-state approximation to the intermediates in eq 12, the following expression for the observed bimolecular ET rate constant (k_{et}) is derived.

$$k_{et} = \frac{k_d}{1 + \frac{k_{-d}}{k_e} + \frac{k_{-d}k_{-e}}{k_{sep}k_e}} \qquad (13)$$

Since the magnitude of k_{sep} can be assumed to be much greater than that of k_{-e}, eq 13 is reduced to

$$k_{et} = \frac{k_d k_e}{k_{-d} + k_e} \qquad (14)$$

If $k_{-d} \ll k_e$, then the k_{et} is given by

$$k_{et} = k_d \qquad (15)$$

and the reaction becomes diffusion controlled. On the other hand, if $k_{-d} \gg k_e$, then k_{et} is represented by

$$k_{et} = \frac{k_d}{k_{-d}}k_e = K_A k_e \qquad (16)$$

In the case of the present system, i.e., the reaction between $^3DMB^*$ and H_{aq}^+, the k_{-d} value is estimated to be 5.9 $\times$ 10^{10} s^{-1} by Eigen equation[46,47]

$$k_{-d} = \frac{3 \times 10^{-3} k_d}{4\pi r_{AB}{}^3 N_A} \qquad (17)$$

The observed ET reaction rate (k_{et} = 7.5 $\times$ 10^6 M^{-1} s^{-1}) is much smaller than the diffusion-controlled rate (5.1 $\times$ 10^{10} M^{-1} s^{-1}), indicating that the relation $k_{-d} \gg k_e$ is applicable. Since the equilibrium constant for the encounter complex formation K_A ($= k_d/k_{-d}$) can be assumed to be unity, one can obtain the following relationship

$$k_{et} = k_e \qquad (18)$$

SCHEME 2

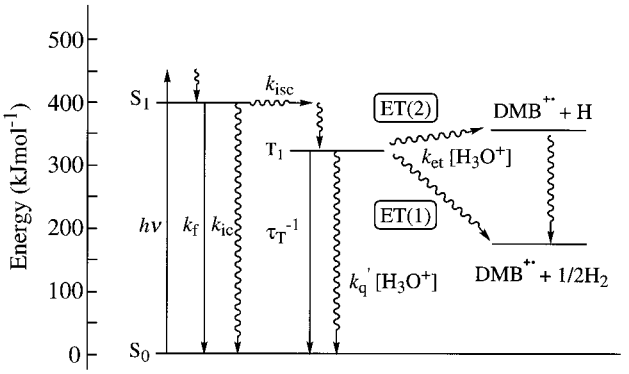

3.6. The Gibbs Free Energy Change (ΔG^0) for the ET Reaction. The Gibbs free energy change ($\Delta G°$) for the ET process between ^{3}DMB* and H_{aq}^+ can be estimated by using electrochemical potentials. If the ET reaction results in $DMB^{+\bullet}$ and hydrogen molecule as shown in eq 19,

$$^3\text{DMB*} + H_{aq}^+ \rightarrow DMB^{+\bullet} + 1/2H_2 \qquad (19)$$

the free energy change can be calculated by[48]

$$\Delta G° = 96.5 \times E^0(DMB^+/DMB) - E_T \qquad (20)$$

where E_T is the triplet energy (325 kJ mol^{-1}) of DMB which was estimated from the phosphorescence spectrum in ethanol glass at 77 K, and $E^0(DMB^+/DMB)$ is the redox potential of DMB. The redox potential of DMB in ACN ($E^0(DMB^+/DMB)_{ACN}$) is reported to be 1.58 eV,[49] which was corrected for the difference in solvation energies in ACN and in aqueous solution by using the following equation:[50−52]

$$E^0(DMB^+/DMB)_{aq} = E^0(DMB^+/DMB)_{ACN} - \frac{(\Delta e)^2}{4\pi\epsilon_0}\frac{1}{2r_D}\left[\frac{1}{\epsilon_{ACN}} - \frac{1}{\epsilon_{H_2O}}\right] \qquad (21)$$

where, $E^0(DMB^+/DMB)_{aq}$ is the oxidation potential of DMB in aqueous solution, ϵ_0 is the dielectric constant in a vacuum, r_D (= 0.37 nm) is the radius of DMB, ϵ_{ACN} (= 36.94) and ϵ_{H_2O} (= 80.16) are the dielectric constants of ACN and water.[42] Thus the $E^0(DMB^+/DMB)_{aq}$ value is obtained to be 1.55 eV, and the overall free energy change for eq 19 is estimated to be −175 kJ mol^{-1}. Therefore, the ET reaction from ^{3}DMB* to H_{aq}^+ is found to become a highly exergonic process if the ET reaction produces the hydrogen molecule as in the case of a standard hydrogen electrode. The thermochemical energy relationship associated with the ET reactions between excited DMB and H_{aq}^+ is shown in Scheme 2.

A more plausible mechanism is shown in Scheme 1(I), where the ET process produces $DMB^{+\bullet}$ and hydrogen atom H_{aq}. $\Delta G_f^0(H_{aq})$ is reported to be 222 kJ mol^{-1},[1,15] which corresponds to the Gibbs free energy change for the conversion ($H_{aq}^+ \rightarrow H_{aq}$) because of the $\Delta G_f^0(H_{aq}^+) = 0$ convention. $\Delta G_f^0(H_{aq})$ includes the hydration free energy change of the hydrogen atom which is estimated to be 19 kJ mol^{-1}.[15,17] In the calculations of ΔG^0 for the ET from ^{3}DMB* to H_{aq}^+, the hydration free energy of hydrogen atom can be neglected. Therefore, the actual free energy change (ΔG^0) for the ET process in Scheme 1(I) can be estimated as follows:

$$\Delta G^0 = 96.5 \times E^0(DMB^+/DMB)_{aq} - E_T + \Delta G_f^0(H) = 28 \text{ kJ mol}^{-1} \qquad (22)$$

The above ΔG^0 value shows the ET reaction from ^{3}DMB* to H_{aq}^+ to be slightly an endergonic process if the ET produces $DMB^{+\bullet}$ and hydrogen atom H (ET(2) in Scheme 2).

In the present experimental conditions, i.e., under relatively low hydronium ion concentrations, the former concerted mechanism (ET(1) in Scheme 2) to produce a hydrogen molecule seems to be an improbable process. Hence it can be expected that the rate of ET reaction from ^{3}DMB* to H_{aq}^+ is governed by the rate of ET(2). The energy relationship depicted in Scheme 2 suggests that the hydrogen atoms produced in ET(2) undergo recombinations to produce hydrogen molecules. The relatively slow ET rate (k_{et} = 7.5 × 10^6 M^{-1} s^{-1}) obtained for the (^{3}DMB* + H_{aq}^+) system is found to be consistent with the $\Delta G°$ value (+28 kJ mol^{-1}) for the ET(2) process.

For the excited singlet state of DMB (^{1}DMB*), $\Delta G°$ for the ET reaction to H_{aq}^+ to produce H was calculated to be −45 kJ mol^{-1} by using the singlet energy of DMB (398 kJ mol^{-1}). The fluorescence of DMB was quenched by H_{aq}^+ with the rate constant of 6.2 × 10^7 M^{-1} s^{-1}, which was about 1 order of magnitude larger than that (7.7 × 10^6 M^{-1} s^{-1}) for ^{3}DMB*. Since the intramolecular charge-transfer character of ^{1}DMB* is considered to be smaller than in the case of anisole and 1-methoxynaphthalene,[20,21] electrophilic protonation to aromatic carbon atoms is not likely for the dominant fluorescence quenching mechanism. The moderately exergonic property for the ET process from ^{1}DMB* to H_{aq}^+ is consistent with the quenching mechanism due to ET from ^{1}DMB* to H_{aq}^+ rather than hydrogen atom exchange reactions at aromatic carbon atoms.

3.7. Isotope Effect. The observed ET rates for the ^{3}DMB*/H_{aq}^+ and ^{3}DMB*/D_{aq}^+ systems in aqueous solution showed a large isotope effect (k_{et}^H/k_{et}^D = 3.0) as described above. The magnitudes of the ET reaction rates (7.5 × 10^6 M^{-1} s^{-1} for H_{aq}^+ and 2.5 × 10^6 M^{-1} s^{-1} for D_{aq}^+) are much smaller than the diffusion-controlled rates. Hence, the isotope effect is not attributable to the difference in the diffusion coefficients of the acceptors (9.0 × 10^{-9} m^2 s^{-1} for H_{aq}^+ 9,12 and 6.66 × 10^{-9} m^2 s^{-1} for D_{aq}^+[53]).

The isotope effects on the ET dynamics have usually been discussed in the light of the changes in the ET parameters such as the driving force ($\Delta G°$), vibrational overlap integrals, inner- (λ_{in}) and outer- (λ_{out}) reorganization energies, etc.[54−60] An approximate quantum mechanical rate expression based on the golden-rule transition probability has been derived for ET systems in the nonadiabatic limit. Nonadiabatic ET for one coupled mode with $h\nu \gg k_BT$ becomes[61,62]

$$k_e = \frac{4\pi^2}{h} H_{RP}^2 \left(\frac{1}{4\pi\lambda_{out} k_B T}\right)^{1/2} (\text{FC}) \qquad (23)$$

$$(\text{FC}) = \sum_{m=0}^{\infty}\left[\frac{e^{-s} S^m}{m!}\right] \exp\left[\frac{-(\lambda_{out} + \Delta G^0 + mh\nu)^2}{4\lambda_{out} k_B T}\right] \qquad (24)$$

where (FC) is Franck−Condon (FC) factor, h is Planck's constant, H_{RP} stands for the electronic matrix element, m is an integer, and

$$S = \lambda_{in}/h\nu \qquad (25)$$

The terms in front of the FC factor in eq 23 are the frequency of ET in the absence of a barrier; this contains H_{RP} and the classical density of states. The FC factor involves $\Delta G°$, λ_{out}, and the sum over all possible vibrational overlap integrals between the initial vibrational level ν and the final level ν'. The isotope effect on vibrational overlap integrals and $\Delta G°$ of an ET process can arise from the zero-point energy effect.[55,56] The origin of the zero-point energy effect can reduce the frequencies of some of the vibrational mode of molecules, and this in turn can reduce the zero-point energy of the deuterated system. Thus, the vibrational overlap integrals between ν and ν' in the FC factor are reduced in D_2O compared with those in H_2O, resulting in an ET reaction rate in D_2O that is slower than in H_2O. In addition, if the reduction in the zero-point energy is greater in the initial state than in the final state, it will cause a reduction in $\Delta G°$ for exergonic ET reactions or an increase in $\Delta G°$ for endergonic ET reactions.

Similar large isotope effects have been reported for some proton-coupled ET reactions.[59,60] The proton-coupled ET reaction contains both the ET and proton transfer.[59,60,63] In the present system, if a proton accepts an electron through the ET reaction, then the structure of $H_9O_4^+$ is broken to produce H_{aq} and $4H_2O$. And this structural change for $H_9O_4^+$ affects the solvent motion beyond the second shell of surrounding solvent molecules.[3] Since the hydrogen bond energy of D_2O is larger than that of H_2O,[55,56,64] the DMB/D_{aq}^+ in the D_2O system should lead to a larger λ_{out} value than that on DMB/H_{aq}^+ in H_2O. This difference in the λ_{out} values would cause the large isotope effect similar to the proton-coupled ET reactions.

4. Concluding Remarks

The ET reaction between excited DMB and the hydronium ion in aqueous solution was investigated by means of the laser photolysis method at 266 nm. The results obtained can be summarized as follows:

(1) DMB in aqueous solution at pH 5.83 is photoionized by two photon absorption processes through the nonrelaxed S_1 state ($S_1^\dagger$) upon 266 nm laser excitation.

(2) Under acidic conditions, the photoionization of DMB occurs through not only the direct photoelectron ejection from higher excited singlet states to water but also through the ET reaction from ^{3}DMB* to the hydronium ion. The ET reaction rate constants are obtained to be 7.5×10^6 M^{-1} s^{-1} for the ^{3}DMB*/H_{aq}^+ system and 2.5×10^6 M^{-1} s^{-1} for the ^{3}DMB*/D_{aq}^+ system, respectively. These relatively small ET rates result from the endergonic nature of the ET reaction ($\Delta G^0 = +28$ kJ mol^{-1}).

(3) The large isotope effect ($k_{et}^H/k_{et}^D = 3.0$) is found for the ET reaction, suggesting that ET reactions contain dissociative properties and that the zero-point energy effects are involved in the ET reaction.

(4) The fluorescence of DMB is quenched by H_{aq}^+ with the rate constant of 6.2×10^7 M^{-1} s^{-1}. The moderately exergonic property for the ET process from ^{1}DMB* to H_{aq}^+ ($\Delta G° = -45$ kJ mol^{-1}) is consistent with the assumption that the fluorescence quenching by H_{aq}^+ is caused, at least in part, by ET to H_{aq}^+.

References and Notes

(1) Bell, R. P. *The Proton in Chemistry*, 2nd ed.; Chapman and Hall: London, 1973.
(2) Komatsuzaki, T.; Ohmine, I. *Chem. Phys*. **1994**, *180*, 239.
(3) Komatsuzaki, T.; Ohmine, I. *Mol. Simulat*. **1996**, *16*, 321.
(4) Ohmine, I.; Tanaka, H. *Chem. Rev*. **1993**, *93*, 2545.
(5) Kobayashi, C.; Iwahashi, K.; Saito, S.; Ohmine, I. *J. Chem. Phys*. **1996**, *105*, 6358.
(6) Minichino, C.; Voth, G. A. *J. Phys. Chem. B* **1997**, *101*, 4544.
(7) Tuckerman, M.; Laasonen, K.; Sprik, M.; Parrinello, M. *J. Phys. Chem*. **1995**, *99*, 5749.
(8) Agmon, N. *Chem. Phys. Lett*. **1995**, *244*, 456.
(9) Green, N. J. B.; Pilling, M. J.; Pimblott, S. M.; Clifford, P. *J. Phys. Chem*. **1990**, *94*, 251.
(10) Goulet, T.; Jay-Gerin, J.-P. *J. Chem. Phys*. **1992**, *96*, 5076.
(11) Shiraishi, H.; Sunaryo, G. R.; Ishigure, K. *J. Phys. Chem*. **1994**, *98*, 5164.
(12) Elliot, A. J.; McCracken, D. R.; Buxton, G. V.; Wood, N. D. *J. Chem. Soc., Faraday Trans*. **1990**, *86*, 1539.
(13) Han, P.; Bartels, D. M. *J. Phys. Chem*. **1992**, *96*, 4899.
(14) Crowell, R. A.; Bartels, D. M. *J. Phys. Chem*. **1996**, *100*, 17713.
(15) Han, P.; Bartels, D. M. *J. Phys. Chem*. **1990**, *94*, 7294.
(16) Natzle, W. C.; Moore, C. B. *J. Phys. Chem*. **1985**, *89*, 2605.
(17) Jortner, J.; Noyes, R. M. *J. Phys. Chem*. **1966**, *70*, 770.
(18) Arnaut, L. G.; Formosinho, S. J. *J. Photochem. Photobiol. A* **1993**, *75*, 1.
(19) Kosower, E. M.; Huppert, D. *Annu. Rev. Phys. Chem*. **1986**, *37*, 127.
(20) Shizuka, H. *Acc. Chem. Res*. **1985**, *18*, 141.
(21) Shizuka, H.; Tobita, S. *J. Am. Chem. Soc*. **1982**, *104*, 6919.
(22) (a) Mann, K. R.; Lewis, N. S.; Miskowski, V. M.; Erwin, D. K.; Hammond, G. S.; Gray, H. B. *J. Am. Chem. Soc*. **1977**, *99*, 5525. (b) Sigal, I. S.; Mann, K. R.; Gray, H. B. *J. Am. Chem. Soc*. **1980**, *102*, 7252.
(23) Suzuki, K.; Tanabe, H.; Tobita, S.; Shizuka, H. *J. Phys. Chem. A.* **1997**, *101*, 4496.
(24) Perichet, G.; Chapelon, R.; Pouyet, B. *J. Photochem.* **1980**, *13*, 67.
(25) Bebelaar, D. *Chem. Phys.* **1974**, *3*, 205.
(26) Bonneau, R.; Carmichael, I.; Hug, G. L. *Pure Appl. Chem.* **1991**, *63*, 289.
(27) Dean, A. J. *Lange's Handbook of Chemistry;* McGraw-Hill, New York, 1973.
(28) Grabner, G.; Monti, S.; Marconi, G.; Mayer, B.; Klein, C.; Köhler, G. *J. Phys. Chem*. **1996**, *100*, 20068.
(29) Braslavsky, S. E.; Heihoff, K. *Handbook of Organic Photochemistry*; Scaiano, J. C., Ed.; CRC Press: Boca Raton, FL, 1989; Vol. 1.
(30) Terazima, M.; Azumi, T. *Chem. Phys. Lett*. **1987**, *141*, 237.
(31) Suzuki, T.; Kajii, Y.; Shibuya, K.; Obi, K. *Chem. Phys*. **1992**, *161*, 447.
(32) Das, P. K.; Encinas, M. V.; Steenken, S.; Scaiano, J. C. *J. Am. Chem. Soc*. **1981**, *103*, 4162.
(33) Paul, S.; Back, M. H. *Can. J. Chem*. **1975**, *53*, 3330.
(34) Baxendale, J. H.; Fielden, E. M.; Capellos, C.; Francis, J. M.; Davies, J. V.; Ebert, M.; Gilbert, C. W.; Keene, J. P.; Land, E. J.; Swallow, A. J.; Nosworthy, J. M. *Nature* **1964**, *201*, 468.
(35) Grabner, G.; Rauscher, W.; Zechner, J.; Getoff, N. *J. C. S. Chem. Comm.* **1980**, 222.
(36) Saito, F.; Tobita, S.; Shizuka, H. *J. Chem. Soc., Faraday Trans.* **1996**, *92*, 4177.
(37) Saito, F.; Tobita, S.; Shizuka, H. *J. Photochem. Photobiol. A*: *Chem.* **1997**, *106*, 119.
(38) (a) Zechner, J.; Köhler, G.; Grabner, G.; Getoff, N. *Chem. Phys. Lett*. **1976**, *37*, 297. (b) Lachish, U.; Ottolenghi, M.; Stein, G. *Chem. Phys. Lett*. **1977**, *48*, 402.
(39) Raz, B.; Jortner, J. *Chem. Phys. Lett*. **1969**, *4*, 155.
(40) Messing, I.; Jortner, J. *Chem. Phys*. **1977**, *24*, 183.
(41) Cockett, M. C. R.; Okuyama, K.; Kimura, K. *J. Chem. Phys*. **1992**, *97*, 4679.
(42) Murov, S. L. *Handbook of Photochemistry*; Marcel Dekker: New York, 1993.
(43) Okada, K.; Yamaji, M.; Shizuka, H. *J. Chem. Soc., Faraday Trans.* **1998**, *94*, 861.
(44) O'Neill, P.; Steenken, S.; Schulte-Frohlinde, D. *J. Phys. Chem*. **1975**, *79*, 2773.
(45) Fielden, E. M.; Hart, E. J. *Rad. Res.* **1967**, *32*, 564.
(46) Eigen, M. Z. *Phys. Chem.* (*Leipzig*) **1954**, *203*, 176.
(47) Marciniak, B.; Bobrowski, K.; Hug, G. L. *J. Phys. Chem.* **1993**, *97*, 11937.
(48) Rehm, D.; Weller, A. *Isr. J. Chem.* **1970**, *8*, 259.
(49) Zweig, A.; Hodgson, W. G.; Jura, W. H. *J. Am. Chem. Soc*. **1964**, *86*, 4124.
(50) Weller, A. *Z. Phys. Chem. N. F*. **1982**, *133*, 93.
(51) Schuster, G. B.; Yang, X.; Zou, C.; Sauerwein, B. *J. Photochem. Photobio. A: Chem*. **1992**, *65*, 191.
(52) Chen, P.; Mecklenburg, S. L.; Meyer, T. J. *J. Phys. Chem*. **1993**, *97*, 13126.
(53) Schmidt, K. H.; Han, P.; Bartels, D. M. *J. Phys. Chem*. **1992**, *96*, 199.
(54) Buhks, E.; Bixon, M.; Jortner, J. *J. Phys. Chem.* **1981**, *85*, 3763.
(55) Weaver, M. J.; Nettles, S. M. *Inorg. Chem*. **1980**, *19*, 1641.

(56) Guarr, T.; Buhks, E.; MoLendon, G. *J. Am. Chem. Soc*. **1983**, *105*, 3763.
(57) Siders, P.; Marcus, R. A. *J. Am. Chem. Soc*. **1981**, *103*, 741, 748.
(58) Reid, P. J.; Silva, C.; Barbara, P. F.; Karki, L.; Hupp, J. T. *J. Phys. Chem.* **1995**, *99*, 2609.
(59) Binstead, R. A.; Stultz, L. K.; Meyer, T. J. *Inorg. Chem*. **1995**, *34*, 546.
(60) Hille, R. *Biochemistry* **1991**, *30*, 8522.
(61) Jortner, J. *J. Chem. Phys*. **1976**, *64*, 4860.
(62) Barbara, P. F.; Meyer, T. J.; Ratner, M. A. *J. Phys. Chem*. **1996**, *100*, 13148.
(63) Cukier, R. I.; Nocera, D. G. *Annu. Rev. Phys. Chem*. **1998**, *49*, 337.
(64) Medhi, K. C.; Kasha, G. S. *Ind. J. Phys*. **1963**, *37*, 139, 275.